Mechanism of indole-3-acetic acid oxidation by plant peroxidases: anaerobic stopped-flow spectrophotometric studies on horseradish and tobacco peroxidases

Irina G. GAZARYAN*, L. Mark LAGRIMINI*, Gillian A. ASHBY† and Roger N. F. THORNELEY†‡

* Department of Horticulture, Ohio State University, Columbus, OH 43210-1096, U.S.A. and †Nitrogen Fixation Laboratory, John Innes Centre, Norwich Research Park, Colney, Norwich NR4 7UH, U.K.

Indole-3-acetic acid (IAA) is a powerful plant growth regulator. The oxidative decarboxylation of IAA by plant peroxidases is thought to be a major degradation reaction involved in controlling the *in vivo* level of IAA. Horseradish peroxidase isoenzyme C and an anionic tobacco peroxidase isolated from transgenic *Nicotiana sylvestris* have been used in experiments *in vitro* designed to determine the mechanism of IAA oxidation. In particular, the initial reduction of ferric to ferrous enzyme, a key step in previously proposed mechanisms, has been investigated by rapid-scan stopped-flow spectrophotometry under strictly anaerobic conditions and at defined oxygen concentrations. The data provide the first evidence for a ternary complex comprising peroxidase, IAA and oxygen that is kinetically competent both at the initiation stage and during the catalytic cycle of IAA oxidation. A general scheme describing the oxidative cycles of both anionic and cationic peroxidases is proposed that includes native ferric enzyme and compound II as kinetically competent intermediates. For anionic peroxidases, addition of hydrogen peroxide switches on the oxidative cycle thereby promoting IAA oxidation. 2-Methyl-IAA is not a substrate of the oxidase reaction, suggesting a specific interaction between plant peroxidases and IAA.

INTRODUCTION

Indole-3-acetic acid (IAA) is a powerful plant growth regulator capable of stimulating cell division and promoting cell elongation at *in vivo* concentrations as low as 10^{-8} M. It is, therefore, important for the plant to control the level of IAA via the regulation of its synthesis and degradation (see [1] and references therein). The oxidative decarboxylation of IAA by plant peroxidases (EC 1.11.1.7) is therefore of considerable physiological importance and has attracted the attention of numerous researchers during the last 40 years (see [2] and references therein). Although it is believed that cationic plant peroxidases play the major role in IAA oxidation [3], the precise physiological relationship between IAA and peroxidases still remains obscure.

Previous mechanistic studies have usually been on horseradish peroxidase isoenzyme C (HRP-C) [2,4–9] and involved steady-state and transient kinetic experiments under aerobic conditions. However, in the earlier studies, turnip peroxidase [4] and horseradish peroxidase isoenzyme A (HRP-A) [5] were also investigated. Two pathways for *in vitro* IAA oxidation by HRP-C have been proposed [6]: (a) the conventional peroxidative cycle (native enzyme → compound I → compound II → native enzyme) operating at high enzyme to substrate ratios and (b) the ferrous enzyme/compound III shuttle (native enzyme → ferrous enzyme → compound III → ferrous enzyme) working at low ratios. The latter scheme is widely accepted though the proposed initiation step, the direct reduction of ferric to ferrous enzyme by IAA, has not been demonstrated experimentally. Recent aerobic stopped-flow studies of the IAA oxidation [2] demonstrated the formation of compound III at high enzyme to substrate ratios but again begged the question about the mechanism of the formation of the ferrous form of HRP-C and its subsequent role in IAA oxidation.

In order to determine whether direct reduction of peroxidase by IAA initiates the oxidation cycle we have studied the reaction by means of anaerobic rapid-scan diode-array stopped-flow spectrophotometry using two plant peroxidases, commercial HRP-C and an anionic tobacco peroxidase (TOP). The latter enzyme was purified after overexpression of its gene in transgenic *Nicotiana sylvestris* plants [10]. The results clearly demonstrate that IAA on its own is unable to reduce these peroxidases directly. Experiments at defined O_2 concentrations show that the initiation step and subseqent IAA oxidation requires a ternary complex comprising ferric enzyme, IAA and oxygen. It is this ternary complex that initiates the generation of the IAA radicals necessary for the oxidative cycle to commence.

MATERIALS AND METHODS

Materials

HRP-C [Type VI; RZ ($A_{403\,nm}/A_{280\,nm} = 3.0$)] was purchased from Sigma and used without further purification. The concentration of HRP-C was determined spectrophotometrically ($\epsilon_{403\,nm} = 102\ mM^{-1}\cdot cm^{-1}$) [11]. IAA (Sigma) and 2-methyl-IAA (Aldrich Chemical Co., U.S.A.) stock solutions were prepared anaerobically under N_2 in 0.1 M Tris/HCl buffer, pH 8.7, and then anaerobically diluted 5-fold with the buffer solution used in each experiment (50 mM sodium citrate, pH 4.5, or 50 mM potassium phosphate, pH 7.0). Aluminium foil wrapping of the serum vials, fitted with rubber closures, was used to minimize photolysis. TOP was purified from transgenic *Nicotiana sylvestris*

Abbreviations used: HRP-C, horseradish peroxidase isoenzyme C; IAA, indole-3-acetic acid; SOD, superoxide dismutase; TOP, tobacco peroxidase.

‡ To whom correspondence should be addressed.

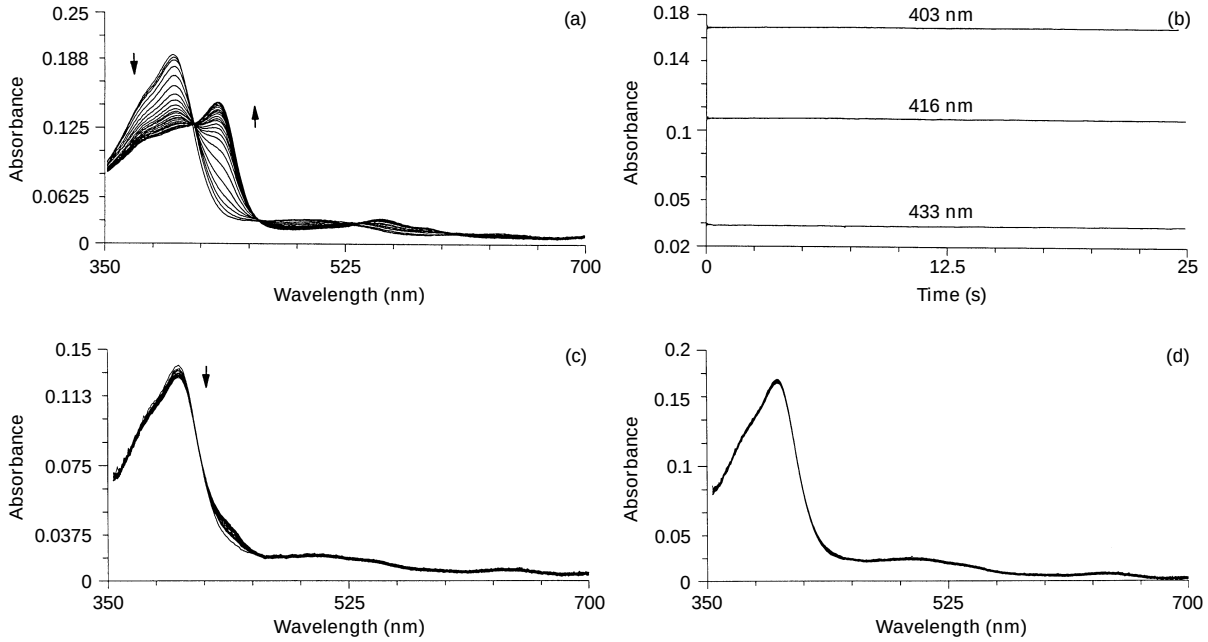

Figure 1 Reaction of HRP-C with IAA in the absence of oxygen showing the effects of xenon lamp-induced photolysis

(**a**) Stopped-flow rapid scans from 0 to 2.4 s with 2.5 mM IAA, 45 mM citrate buffer, pH 4.5. (**b**) Stopped-flow traces at 403, 416 and 433 nm under single-wavelength conditions (tungsten lamp): 5 mM IAA, 45 mM citrate buffer, pH 4.5. (**c**) Stopped-flow rapid scans from 0 to 24 s with 5 mM IAA, 45 mM citrate buffer, pH 4.5. (**d**) Stopped-flow rapid scans from 0 to 24 s with 5 mM IAA, 45 mM phosphate buffer, pH 7.0. All the reactions were measured at 25 °C with 2 μM HRP, 10 mM Tris/HCl. In experiments (**c**) and (**d**) a 360 nm filter was used to prevent UV-photolysis of the reactants. Arrows indicate the direction of the absorbance changes with time.

plants as follows: 1 kg of leaves was collected just before flowering, homogenized in 2 l of 0.1 M Tris/HCl buffer, pH 6.0, filtered and centrifuged (25000 ***g***, 20 min). The supernatant (3.5 l) was treated with DEAE-cellulose to remove pigments, then diluted 10 times with distilled water and applied to DEAE-cellulose equilibrated with 0.01 M Tris/HCl buffer, pH 6.0. The enzyme was eluted in 0.1–0.15 M Tris/HCl buffer, pH 6.0, and then run on a Sephacryl S-200 column (5 cm × 100 cm) in 0.01 M Tris/HCl buffer, pH 6.0. The active fractions were collected, concentrated to 10 mg/ml, sterilized by filtration and stored at 4 °C. The homogeneous enzyme preparation obtained (yield 60 mg) had a molecular mass of 36 kDa and a pI of 3.5 [7]. The RZ value was in the range 3.4–3.8. The concentration of TOP was determined spectrophotometrically assuming an ϵ_{403nm} of 108 $mM^{-1} \cdot cm^{-1}$.

Methods

Anaerobic stopped-flow studies were performed using a Hi-Tech SF-61 rapid-scan stopped-flow spectrophotometer equipped with xenon lamp and in single-wavelength mode with a tungsten lamp. The single-wavelength experiments were performed at 403 nm (maximum for the ferric enzyme), 416 nm (maximum of compound II absorbance, the isosbestic point between ferric and ferrous forms), and 433 nm (the maximum of the ferrous form, the isosbestic point between ferric enzyme and compound I). The stopped-flow apparatus was installed in an anaerobic glove box operating under N_2 with less than 1 p.p.m. of O_2. Enzyme stock solutions and the buffers were deoxygenated for 30 min before being placed into the glove box. Air- or oxygen-saturated buffer was placed into the anaerobic box in hermetically sealed serum vials. Oxygen concentrations were varied in the range 10–600 μM by premixing the air- or oxygen-saturated buffer with the deoxygenated buffer in syringes with no gas head space to avoid loss of O_2 from the solutions.

IAA and 2-methyl-IAA degradation products were characterized by reverse-phase HPLC using a Hewlett–Packard HP1090 Liquid Chromatograph with a UV detector (254 nm). Reaction mixtures containing IAA or 2-methyl-IAA (200 μM) and TOP (0.07 μM) in sodium acetate buffer (100 mM, pH 5.0) were incubated at 24 °C for 10 min in the presence and absence of O_2. Aliquots were analysed by isocratic elution in a methanol/1 % acetic acid mixture (40:60, v/v) on a Supelcosil LC-18-DB column (150 mm × 4.6 mm; Supelco, Bellefonte, U.S.A.). Peaks were identified by comparison of retention times with those of authentic samples of 2,3-dimethylindole, indole-3-carbinol, indole-3-aldehyde and 2-methylindole-3-aldehyde (Aldrich, U.S.A.) made up in methanol. H_2O_2 (2 mM) was added to the TOP/2-methyl-IAA reaction mixture after 1 h incubation.

RESULTS

In early experiments, rapid-scan stopped-flow data for the reaction of HRP-C with IAA under strictly anaerobic conditions showed the direct reduction of the ferric enzyme to the ferrous state (Figure 1a). However, when similar experiments were conducted using a tungsten lamp with single-wavelength monitoring (403, 416 and 433 nm, Figure 1b), no reaction was detected. It was concluded that the high-intensity xenon lamp was causing significant photolysis of the reactants. The use of a 360 nm filter between the xenon lamp and the observation chamber in subsequent rapid-scan experiments essentially eliminated this photolysis with only traces of the ferrous form of the enzyme being detected (Figure 1c). At pH 7.0, no ferrous enzyme was detected

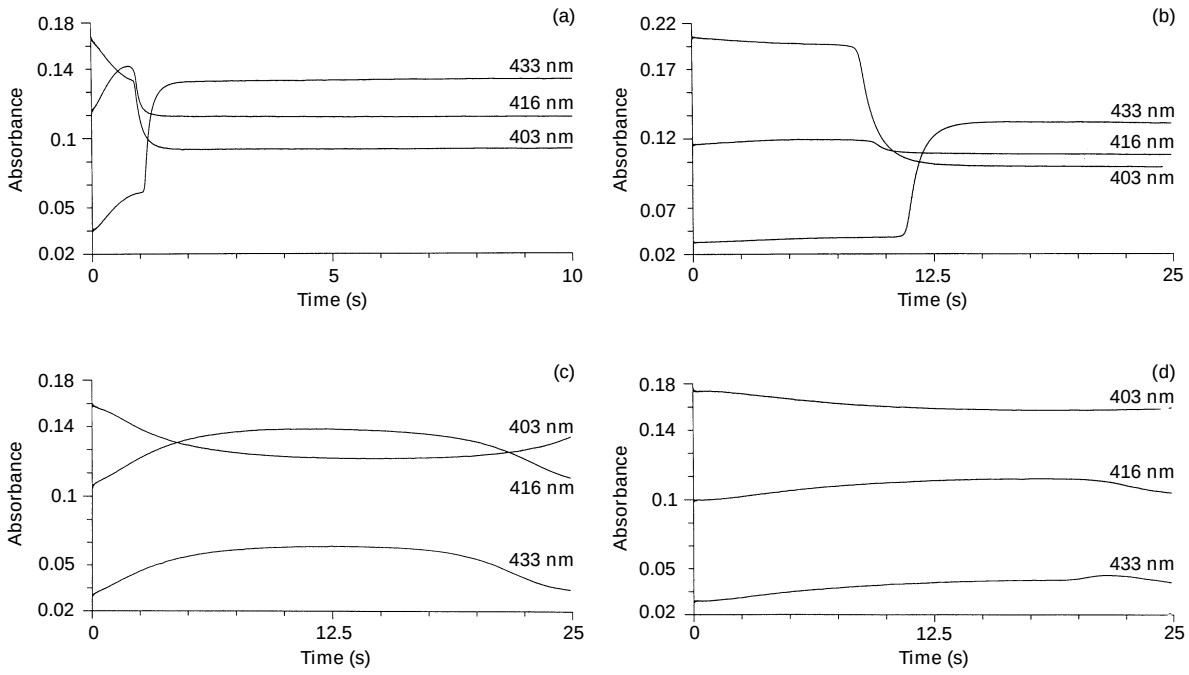

Figure 2 Stopped-flow absorbance changes under single-wavelength conditions (tungsten lamp) for the reactions of HRP-C and TOP with IAA and dioxygen

(**a**) 2 μM HRP, 45 mM citrate buffer, pH 4.5. (**b**) 2 μM TOP, 45 mM citrate buffer, pH 4.5. (**c**) 2 μM HRP, 45 mM phosphate buffer, pH 7.0. (**d**) 2 μM TOP, 45 mM phosphate buffer, pH 7.0. All the reactions were measured at 25 °C with 5 mM IAA, 10 mM Tris/HCl, 62.5 μM O_2 at 403 nm, 416 nm and 433 nm.

in rapid-scan experiments when a 360 nm filter was employed (Figure 1d). Similar results were obtained for TOP (results not shown).

Thus, under strictly anaerobic conditions both peroxidases were reduced to their ferrous forms by IAA only when xenon lamp-induced photolysis was occurring. This reduction was sensitive to pH, indicating the involvement of radical species produced in higher concentrations at low pH values. On account of this photolysis phenomenon, all subsequent experiments were performed either at single wavelengths with a tungsten lamp or with a 360 nm filter fitted to the xenon lamp for rapid-scan stopped-flow spectrophotometry.

Single-wavelength stopped-flow data at fixed oxygen levels clearly demonstrate a reaction between both the peroxidases and IAA. The absorbance changes were recorded at 403, 416 and 433 nm at pH 4.5 and 7.0 (Figure 2). These data show distinct differences between the reactivities of HRP-C and TOP at pH 4.5. In the case of TOP (Figure 2b) only very small spectral changes were recorded during a lag period of approx. 10 s. The length of this lag phase was proportional to the oxygen concentration. HRP-C (Figure 2a) exhibited biphasic kinetics and again the duration of the first phase was proportional to the oxygen concentration. The duration of the first phase in the case of HRP-C was much shorter than for TOP at pH 4.5, indicating nearly an order of magnitude higher rate of oxygen consumption for HRP-C. At pH 7.0, the rates of oxygen consumption for TOP and HRP-C were comparable. The rapid-scan data shown in Figures 3(a) and 3(b) emphasize the differences between HRP-C and TOP at pH 4.5 and show that different redox states of the enzymes are present in each kinetic phase. In the case of HRP-C, compound III was formed in the first kinetic phase followed by ferrous enzyme. Compound III has characteristic peaks in the visible region (543 and 581 nm) distinguishing it from compound

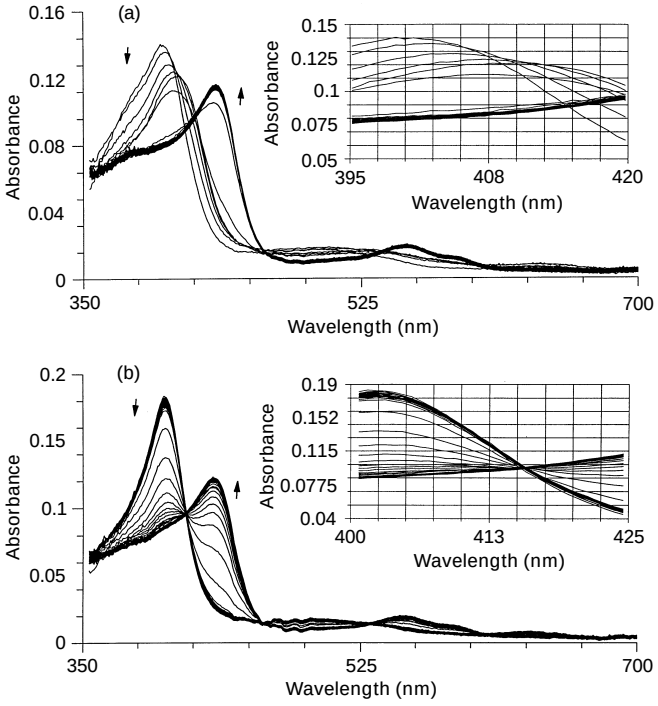

Figure 3 Stopped-flow rapid-scan time courses comparing the reactions of HRP-C and TOP with IAA and dioxygen at pH 4.5

Rapid-scan data from 0 to 24 s using a 360 nm filter to prevent UV photolysis. Comparison of (**a**) HRP and (**b**) TOP. The inserts show a 25 nm scan around the isosbestic points. All reactions were measured at 25 °C and contained 2 μM peroxidase, 5 mM IAA, 62.5 μM O_2, 10 mM Tris/HCl, 45 mM citrate buffer, pH 4.5. The arrows indicate the direction of the change in absorbance with time.

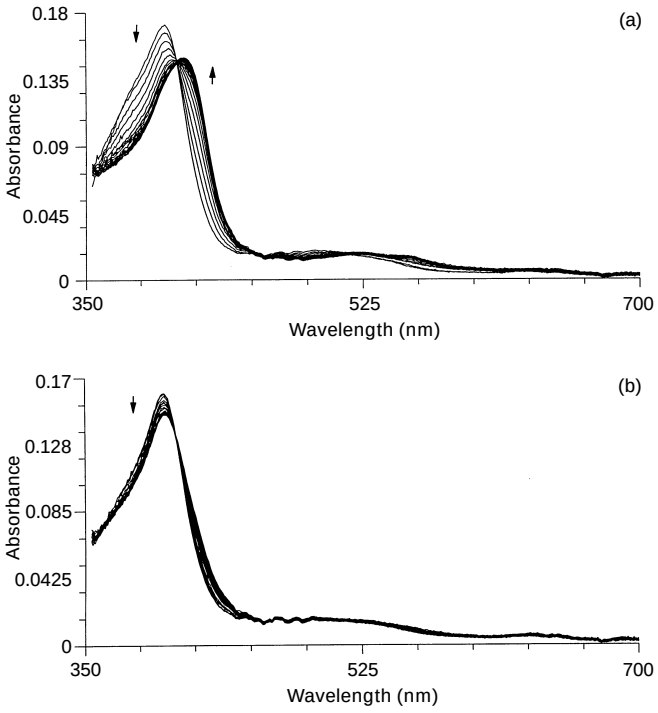

Figure 4 Stopped-flow rapid-scan time courses comparing the reactions of HRP-C and TOP with IAA and dioxygen at pH 7.0

Rapid-scan data from 0 to 24 s using a 360 nm filter to prevent UV photolysis. Comparison of (**a**) HRP and (**b**) TOP. Reactions were measured at 25 °C with 2 μM peroxidase, 5 mM IAA, 62.5 μM O_2, 10 mM Tris/HCl, 45 mM phosphate buffer, pH 7.0. The arrows indicate the direction of the change in absorbance with time.

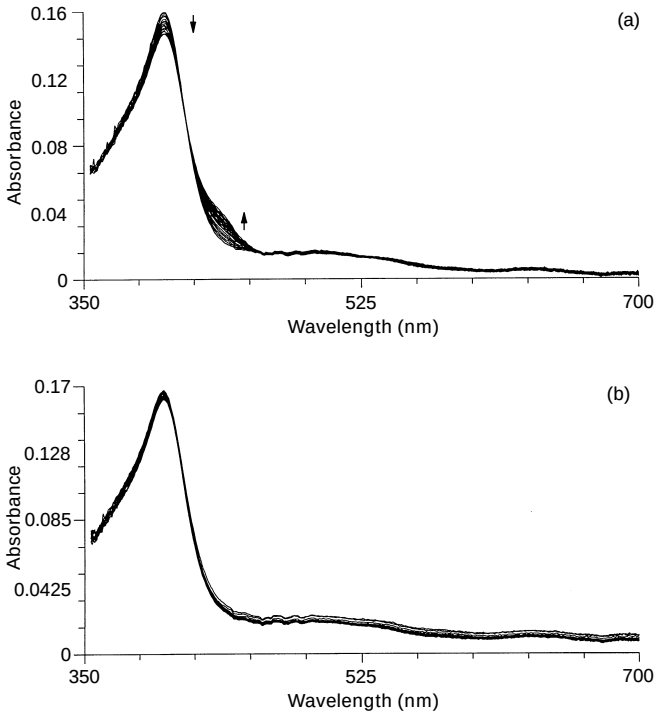

Figure 5 Stopped-flow rapid-scan time courses for the reaction of TOP with 2-methyl-IAA and dioxygen at pH 4.5

Rapid-scan data from 0 to 24 s using 360 nm filter to prevent UV photolysis showing the reaction of TOP (2 μM) with 2-methyl-IAA (5 mM) in (**a**) the absence of O_2 and (**b**) with 62.5 μM O_2. The reactions were measured at 25 °C with 10 mM Tris/HCl, 45 mM citrate, pH 4.5. The arrows indicate the direction of the change in absorbance with time.

II (527 and 557 nm). No defined isosbestic point between native enzyme and compound III (408–410 nm, see the insert to Figure 3a) was observed, indicating that compound II might be formed during this sequence of reactions (see also the Discussion section). TOP showed no spectral changes during the lag phase before the ferrous enzyme appeared with a clearly defined isosbestic point at 416 nm (see the insert to Figure 3b). However, with both enzymes, the ferrous forms only appeared after all the oxygen had been consumed. At pH 7.0, both peroxidases behaved similarly, the native forms being directly converted into compound II with a clearly defined isosbestic point at 408 nm (Figures 4a and 4b). At longer times compound II was converted back into the native form. No ferrous enzyme species was detected.

The ability of 2-methyl-IAA to reduce peroxidases in the absence of oxygen was similar to IAA (Figure 5a), but is attributed to a photolysis effect seen in the absence of the 360 nm filter since no absorbance changes were seen with the tungsten lamp in single-wavelength experiments. In the presence of oxygen, again no spectral changes were recorded (compare Figure 5b with Figure 3b). Thus, 2-methyl-IAA is not a substrate for the oxidase reaction though radicals derived from it under conditions when photolysis occurs gave rise to a small amount (approx. 10%) of the ferrous form of the enzyme. HPLC was used to measure residual 2-methyl-IAA and IAA and to identify any degradation products. 2-Methyl-IAA was stable for hours at pH 5.0 in the presence of TOP, whereas IAA was completely degraded in 10 min under the same conditions. Degradation of 2-methyl-IAA was only observed after the addition of H_2O_2 (2 mM) with 2-methyl-3-aldehyde and 2,3-dimethylindole as identifiable products of the peroxidative reaction. The formation of 2,3-dimethylindole strongly suggests a radical mechanism for 2-methyl-IAA peroxidation [12].

These results mean that: (1) IAA does not reduce peroxidases directly under strictly anaerobic conditions; (2) ferric enzyme is reduced non-specifically to the ferrous state by radicals derived from IAA and 2-methyl-IAA following photolysis at low pH; (3) spectral changes not related to photolysis are induced only when oxygen is present; (4) 2-methyl-IAA is not a substrate for peroxidase in the oxidative cycle; and (5) pH plays a key role in both the enzymic and photolytic reactions.

Scheme 1 is able to explain these observations.

DISCUSSION

In this study we have shown for the first time that IAA is unable to reduce peroxidase directly under anaerobic conditions except by light-induced radical production. Therefore, the widely accepted scheme described by eqns. (1), (2) and (3) [2,6] which requires the direct reduction of ferric enzyme by IAA to initiate the cycle (eqn. 1) has to be reconsidered.

$$E^{3+} + IAA \rightarrow E^{2+} + IAA^{\bullet +} \quad (1)$$

$$E^{2+} + O_2 \rightarrow \text{compound III} \quad (2)$$

$$\text{Compound III} + IAA \rightarrow E^{2+} + CO_2 + H_2O + \text{indole-aldehyde} \quad (3)$$

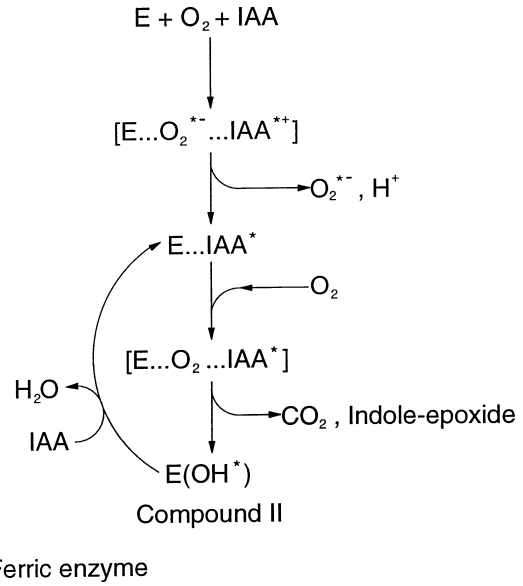

Scheme 1

Strong evidence for ferrous enzyme formation via secondary radical processes is our observation that UV light induces the reduction of HRP-C and TOP in the presence of IAA (Figures 1a and 1c) and 2-methyl-IAA (Figure 5a). The reduction of the ferric enzymes to their ferrous states appears to be a light-induced non-specific reaction because 2-methyl-IAA is not a substrate for the oxidase reaction (Figure 5b) and is only able to reduce the enzyme under conditions of high UV-light intensity. The pH-dependence of this reaction probably reflects the pH-dependence of the redox potential for the ferric/ferrous peroxidase couple. At low pH, peroxidases have a higher mid-point potential. Radical species capable of effecting the reduction are also more likely to be produced at low pH (see discussion below). The reduction of ferric to ferrous enzyme can occur via the reaction described by eqn. (4) first proposed by Nakajima and Yamazaki [5]:

$$E^{3+} + IAA^{\bullet} \rightarrow E^{2+} + IAA^{+} \quad (4)$$

where the $IAA^{\bullet}$ radical species is most likely a skatole radical formed by spontaneous decarboxylation of IAA.

What then initiates the oxidative cycle if ferrous enzyme is only a secondary product of a light-induced reaction? The anaerobic stopped-flow data obtained for the first time in this study demonstrate that pronounced spectral changes are induced only when oxygen is added to the IAA–enzyme system. The initiation step of IAA oxidation must proceed via a ternary complex involving native enzyme, oxygen and IAA (see below the reasoning against two sequential reactions based on the failure of 2-methyl-IAA to act as a substrate for the oxidative cycle). The data on IAA oxidation by HRP at low pH support the hypothesis that the reaction starts via a ternary complex resulting in compound III and $IAA^{\bullet+}$ cation radical formation (eqn. 5).

$$E^{3+} + IAA + O_2 \rightarrow \text{compound III} + IAA^{\bullet+} \quad (5)$$

However, the data obtained for IAA oxidation by TOP both at low and neutral pH and by HRP-C at pH 7.0 can only be rationalized by a general scheme that includes the formation of an intermediate ternary complex (eqn. 6) that gives rise to superoxide anion-radical (eqn. 7):

$$E^{3+} + O_2 + IAA \rightarrow [E^{3+}\text{–}O_2^{\bullet-}\text{–}IAA^{\bullet+}] \quad (6)$$

$$[E^{3+}\text{–}O_2^{\bullet-}\text{–}IAA^{\bullet+}] \rightarrow E^{3+} + O_2^{\bullet-} + IAA^{\bullet+} \quad (7)$$

The superoxide anion-radical produced reacts with HRP forming compound III (eqn. 8):

$$E^{3+} + O_2^{\bullet-} \rightarrow \text{compound III} \quad (8)$$

It is well known that superoxide radical is produced in the course of IAA oxidation [2,8] by O_2 and peroxidase with $IAA^{\bullet+}$ as the primary radical product [8]. It has been shown recently [2] that superoxide dismutase (SOD) inhibits HRP-C compound III formation in this reaction. Thus in the case of HRP-C two mechanisms of compound III formation may operate: mechanism A, via the ternary interaction shown in eqn. (5); and mechanism B, via ferric enzyme interacting with superoxide anion (eqn. 8) derived from an intermediate ternary complex (eqns. 6 and 7). For TOP, only mechanism B (eqns. 6 and 7) operates since no compound III formation is observed at high or low pH.

Mechanisms A and B (eqns. 5 and 7 respectively) both require a ternary complex involving enzyme, oxygen and IAA for oxygenase activity (i.e. direct activation of molecular oxygen). We emphasize that IAA oxidation is sensitive to minor changes in the substrate structure. In the present study, we have shown that addition of a methyl group to IAA at position 2 of the indole ring greatly decreases the activity of the oxidation cycle although 2-methyl-IAA was a good substrate for the peroxidase cycle. Candeias et al. [12] have recently shown that 2-methyl-IAA is a peroxidase substrate of HRP-C. Although 2-methyl-IAA spontaneously produces radicals under aerobic conditions in water or methanol, it clearly does not participate in the peroxidase-catalysed oxidative cycle. The mechanism recently proposed by Krylov and Dunford [13], based on the formation of $IAA^{\bullet}$ radicals during the induction phase, cannot explain the failure of 2-methyl-IAA to function as a peroxidase substrate in the oxidase cycle. 2-Methyl-IAA is non-enzymically more readily converted into a radical species than is IAA under aerobic conditions. Therefore, according to the Krylov and Dunford mechanism [13], 2-methyl-IAA should be a better oxidase cycle substrate than IAA. This is clearly not consistent with the observations reported in this paper. Similar effects have been reported previously for indole-3-propionate [7], indole-3-butyrate [7], α,α-dimethyl-IAA [14] and in this study 2-methyl-IAA. *N*-Methyl-IAA is the only exception, to our knowledge [7]. We conclude that this specificity for IAA in the oxidase reaction may indicate a specific binding site for IAA on plant peroxidases. Our transient kinetic data, with controls under strictly anaerobic conditions, provide the first direct evidence for a ternary complex comprising a peroxidase, IAA and dioxygen. The formation of this complex is highly dependent on substrate structure (2-methyl-IAA is not a substrate) and is essential for IAA oxidation by plant peroxidases.

The formation of $IAA^{\bullet+}$ cation radicals via the ternary interactions shown in eqns. (5) and (7) readily explains the effect of pH on the kinetics of the reaction. The properties of $IAA^{\bullet+}$ cation-radical are strongly pH-dependent according to the recent report by Candeias et al. [12]. The $IAA^{\bullet+}$ cation radical rapidly decarboxylates (eqn. 9) with a first-order rate constant of $1.8 \times 10^4\ s^{-1}$. However, at neutral pH it rapidly converts into the indolyl radical after release of a proton ($pK_a = 5.1$). The indolyl radical decarboxylates much more slowly ($k < 100\ s^{-1}$). At neutral pH, binary interactions dominate the chemistry of $IAA^{\bullet+}$

cation radicals. Therefore IAA enzymic oxidation at low pH predominantly results in the formation of skatole radicals, whereas at neutral pH indolyl radicals are the main species involved. Skatole radicals can also be produced non-enzymically and initiate a number of radical reactions that may occur concurrently with the enzymic process and complicate any detailed kinetic analysis.

$$IAA^{\bullet+} \rightarrow \text{indole-3-}CH_2^{\bullet}\ (\text{skatole radical}) + CO_2 \quad (9)$$

$$\text{Indole-3-}CH_2^{\bullet} + O_2 \rightarrow \text{indole-3-}CH_2O_2^{\bullet} \quad (10)$$

$$\text{Indole-3-}CH_2O_2^{\bullet} + IAA \rightarrow \text{indole-3-}CH_2OOH\ (\text{skatole hydroperoxide}) + IAA^{\bullet} \quad (11)$$

The appearance of IAA hydroperoxide via reaction (11) could switch the peroxidative cycle on. However, it also could decompose non-enzymically producing an intermediate slowly converting into methylene-oxindole [5].

The second catalytic step in the proposed mechanism of IAA oxidation is related to the formation of compound II observed in this study at pH 7.0 and in previous studies at low pH values [4–6]. At pH 4.5 we did not observe a clearly defined isosbestic point between HRP-C compound III and ferric enzyme (Figure 3a). The same observation was reported in earlier stopped-flow studies under aerobic conditions [2]. This can be explained by the presence of compound II, since its reactivity towards IAA is about two orders of magnitude higher than that of compound III (the second-order reaction rate constants are $1.8 \times 10^4\ M^{-1} \cdot s^{-1}$ and $710\ M^{-1} \cdot s^{-1}$ respectively [15]). In the case of TOP the rapid-scan data at pH 4.5 showed that native ferric enzyme is the major form present during oxygen consumption (lag phase approx. 10 s). In the single-wavelength experiments (Figure 2b) some minor changes in absorbance at 403, 416 and 433 nm were observed, indicating the formation of some TOP compound II which is known to be extremely active in acidic medium [16].

If compound II is the key enzyme intermediate responsible for IAA oxidation in the presence of oxygen, as has been previously proposed [4,5] and which is also evident from the data obtained at neutral pH in this study, its formation should follow the initiation step of the reaction and be the rate-limiting step for the whole cycle of IAA oxidation. The lag periods for compound II formation observed in this study (Figure 2d) and in one previous study [5] show that compound II is formed only after an induction period. A reaction sequence for compound II formation during IAA oxidation has been proposed by Ricard and Job [4] who also suggested the formation of a ternary complex between ferric enzyme, IAA radical and oxygen (eqn. 12).

$$E^{3+}\text{–}IAA^{\bullet} + O_2 \rightarrow E^{3+}(OH^{\bullet})\ (\text{compound II}) + CO_2 + \text{indole-epoxide} \quad (12)$$

$$E^{3+}(OH^{\bullet}) + IAA \rightarrow E^{3+}\text{–}IAA^{\bullet} + H_2O \quad (13)$$

The $IAA^{\bullet}$ radical is most likely an indolyl radical which is known not to decarboxylate [12].

The stimulation of compound II formation [2] by the addition of SOD is consistent with the dissociation of O_2^- from the third form of the ternary complex shown in eqn. (6) to yield a ferric enzyme–$IAA^{\bullet+}$ complex as shown in eqn. (14).

$$[E^{3+}\text{–}IAA^{\bullet+}\text{–}O_2^{\bullet-}] \rightarrow E^{3+}\text{–}IAA^{\bullet} + H^+ + O_2^{\bullet-} \quad (14)$$

The removal of superoxide radical by SOD will shift the equilibrium to the right, increasing the amount of the E^{3+}–$IAA^{\bullet+}$ complex and thereby increasing the amount of compound II via the reaction shown in eqn. (12).

A comparison of the duration of the lag period observed for TOP at pH 4.5 (approx. 10 s) with the duration of the TOP–TOP compound II–TOP cycle at pH 7.0 (30 to 40 s) indicates that the activity of TOP compound II decreases 4-fold in neutral medium. However, even at pH 7.0 it is still very high compared with that of HRP compound II as shown by the comparable rates of oxygen consumption (approx. 30 and 25 s in Figures 2d and 2c respectively). The rapid-scan data show essentially complete conversion of HRP into compound II (Figure 4a) whereas TOP is present mainly in the ferric form (Figure 4b). The duration of the lag period is determined by the initial oxygen concentration. On exhaustion of oxygen at pH 4.5, ferrous enzyme is formed, while at pH 7.0 compound II reverts to native enzyme. However, for HRP-C the time to exhaust the oxygen at pH 4.5 is an order of magnitude less than at pH 7.0 (1–2 s and 30 s respectively). The only way to explain the difference between HRP-C and TOP is to consider the formation of HRP-C compound III as the main factor that stimulates IAA oxidation and oxygen consumption. A direct two-electron reduction of HRP-C compound III to compound II was observed at low temperatures by Ricard and Job [4]. Such a reaction could be the best explanation for this stimulation phenomenon. This reaction also provides an additional route for compound II formation and consequent promotion of IAA oxidation. Our kinetic and spectroscopic evidence for a ternary interaction between peroxidase, IAA and oxygen with a unique binding site for IAA (2-methyl-IAA is excluded) implies that this site is sufficiently close to the haem iron for direct oxygen transfer to IAA to occur. This seems more likely to us than the simultaneous binding of two IAA molecules on the enzyme as proposed by Ricard and Job [4].

$$E^{3+}(OOH^{\bullet})\ (\text{compound III}) + IAA \rightarrow E^{3+}(OH^{\bullet})\ (\text{compound II}) + IAAOH \quad (15)$$

TOP does not form compound III and therefore the reaction shown in eqn. (15) cannot be part of its oxidative cycle. In this case only the addition of H_2O_2 could give the additional route to compound II via the peroxidative cycle. Indeed, the stimulation of oxygen consumption by the H_2O_2 with the elimination of the lag phase was first described for anionic TOP [17] and subsequently for HRP-A [5].

Conclusions

(1) Spectrophotometric and stopped-flow kinetic data obtained under strictly anaerobic conditions are best interpreted in terms of a ternary interaction involving enzyme, IAA and dioxygen both at the initiation stage and during the catalytic cycle of IAA oxidation by plant peroxidases. A general scheme describing the oxidative cycles of both anionic and cationic peroxidases is proposed that includes the native enzyme and compound II states as kinetically competent intermediates (Scheme 1).

(2) Superoxide radical and $IAA^{\bullet+}$ cation radical are formed in the initial reaction.

(3) Compound II is formed when enzyme-bound $IAA^{\bullet+}$ and O_2 react.

(4) 2-Methyl-IAA is not a substrate of the oxidase reaction although it is a substrate for the peroxidase cycle.

(5) The oxidative cycle must function independently of the peroxidase cycle. This is consistent with the results of chemiluminescence studies on the same systems [8].

(6) For cationic peroxidases, compound III provides an additional route for compound II formation and stimulates the oxidative cycle.

(7) For anionic peroxidases, addition of H_2O_2 switches on the oxidative cycle thereby promoting IAA oxidation.

We conclude that plant peroxidases in their reactions with IAA behave like oxygenases with high substrate specificity. IAA appears to be a unique substrate for plant peroxidases, suggesting

that its oxidation may be an important physiological role for plant peroxidases.

We thank Professor H. B. Dunford and Dr. L. P. Candeias for their helpful comments on the manuscript.

REFERENCES

1 Nilsson, O., Crozier, A., Schmulling, T., Sandberg, G. and Olsson, O. (1993) Plant J. **3**, 681–689
2 Metodiewa, D., Pires de Melo, M., Escobar, J. A., Cilento, G. and Dunford, H. B. (1992) Arch. Biochem. Biophys. **296**, 27–33
3 Gaspar, T., Penel, C., Castillo, F. J. and Greppin, H. (1985) Physiol. Plant **64**, 418–423
4 Ricard, J. and Job, D. (1974) Eur. J. Biochem. **44**, 359–374
5 Nakajima, R. and Yamazaki, I. (1979) J. Biol. Chem. **254**, 872–878
6 Smith, A. M., Morrison, W. L. and Milham, P. J. (1982) Biochemistry **21**, 4414–4419
7 Kobayashi, S., Sugioka, K., Nakano, H., Nakano, M. and Tero-Kubota, S. (1984) Biochemistry **23**, 4589–4597
8 Pires de Melo, M., Escobar, J. A., Metodiewa, D., Dunford, H. B. and Cilento, G. (1992) Arch. Biochem. Biophys. **296**, 34–39
9 Acosta, M., del Rio, J. A., Arnao, M. B., Sanchez-Bravo, J., Sabater, F., Garcia-Carmona, F. and Garcia-Canovas, F. (1988) Biochim. Biophys. Acta **955**, 194–202
10 Lagrimini, L. M., Burkhart, W., Moyer, M. and Rothstein, S. (1987) Proc. Natl. Acad. Sci. U.S.A. **84**, 7542–7547
11 Ohlsson, P.-I. and Paul, K. G. (1976) Acta Chem. Scand. **B30**, 373–375
12 Candeias, L. P., Folkes, L. K., Porssa, M., Parrick, J. and Wardman, P. (1995) Free Radical Res. **23**, 403–418
13 Krylov, S. N. and Dunford, H. B. (1995) Biophys. Chem. **2105**, in the press
14 Hinman, R. L. and Lang, J. (1965) Biochemistry **4**, 144–158
15 Yamazaki, I and Yokota, K. (1973) Mol. Cell. Biochem. **2**, 39–45
16 Gazaryan, I. G. and Lagrimini, L. M. (1995) Phytochemistry, in the press
17 Sequeria, L. and Mineo, L. (1966) Plant Physiol. **41**, 1200–1208

Received 10 July 1995/18 September 1995; accepted 21 September 1995